Conformation-Dependent Intramolecular Electron Transfer in *N*-(Aminoalkyl)-9-phenanthrenecarboxamides

Frederick D. Lewis* and Eric L. Burch

Department of Chemistry, Northwestern University, 2145 Sheridan Road, Evanston, Illinois 60208-3113

Received: September 13, 1995; In Final Form: November 12, 1995[⊗]

The molecular structure and photophysical behavior of several secondary and tertiary *N*-(aminoalkyl)-phenanthrenecarboxamides have been investigated. Secondary (aminoalkyl)amides exist predominantly in the *Z* conformation, whereas tertiary amides exist as mixtures of *Z* and *E* conformers and semirigid piperazines as mixtures of chair conformers. Rate constants for endergonic intramolecular electron transfer are found to be highly dependent upon molecular structure. The aromatic and amide groups of the tertiary amides are essentially orthogonal, and thus, an *E* aminoalkyl group can adopt low-energy conformations in which there is spatial overlap between the aromatic and amine groups, whereas such overlap is not possible for either a *Z* aminoalkyl group or the piperazines. The observation of more rapid intramolecular electron transfer quenching of the phenanthrene singlet by an appended trialkylamine in the *E* vs *Z* conformation is attributed to this difference in overlap. An increase in the phenanthrene−amide dihedral angle is also found to result in a decrease in the rate constant for intramolecular electron transfer quenching by a *Z* aminoalkyl group. In the case of appended tertiary anilines, efficient electron transfer quenching occurs for both *Z* and *E* conformers. The *Z* conformers form fluorescent exciplexes, providing a new example of exciplex-type emission in the absence of direct $\pi-\pi$ overlap. Exciplexes formed by the *E* conformers are nonfluorescent and apparently undergo rapid intersystem crossing. The strong exciplex emission observed at low temperatures both in solution and in frozen glasses is attributed to ground state dimers or aggregates.

Introduction

Formation of an amide linkage provides a simple method of connecting small molecular building blocks to form larger molecules. In addition to its function as a linker, the amide group can also serve as a conformational control element.[1] Amides with two different substituents on nitrogen exist as mixtures of *Z* and *E* conformational isomers. Most secondary amides (R_2 = H) exist predominantly in the *Z* conformation (eq 1); whereas tertiary amides exist as mixtures of *Z* and *E* isomers, with rotational barriers generally in excess of 15 kcal/mol. In the case of aromatic carboxamides, the arene−carbonyl dihedral angle, φ_1, is dependent upon the steric demands of the arene. Amide−arene resonance favors a small value of φ_1 for benzamides (<30°), whereas nonbonded repulsion can result large values of φ_1 (>60°), as in the case of 9-phenanthrenecarboxamides.[1,2] The amide group remains planar ($\varphi_2 \sim 0°$) even in the tertiary amides of sterically demanding aromatic carboxamides.

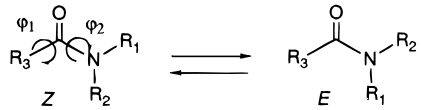

(1)

The amide group has been employed in investigations of photoinduced electron transfer as a linker in the construction of diad and triad molecules.[3,4] However, the effect of the amide's distinct conformational preferences upon electron transfer processes has not been investigated. We report here the results of our investigations of intramolecular quenching of the fluorescent states of the singlet *N*-(aminoalkyl)-9-phenanthrenecarboxamides. For purposes of comparison, intermolecular quenching of the model compounds **1**, **4**, and **13** by amines has also been investigated. The aminoalkyl groups in the secondary amides **2** and **3** exist predominantly in the *Z* configuration, whereas the tertiary amides **5**−**10** exist as mixtures of *E* and *Z* isomers that interconvert slowly on the excited state time scale. This permits comparison of intermolecular quenching by *Z* vs *E* isomers as functions of aminoalkyl chain length (**6** vs **7**) and amine oxidation potential (**6** vs **8** and **6** vs **9**).[5] The effect of the dihedral angle φ_1 upon intramolecular electron transfer quenching can be investigated by comparison of the results for the lactam **14**, secondary amide **2**, and tertiary amides **6**. Finally, the effects of restricted conformational mobility have been probed for the semirigid piperazines **11** and **12**.

CHART 1

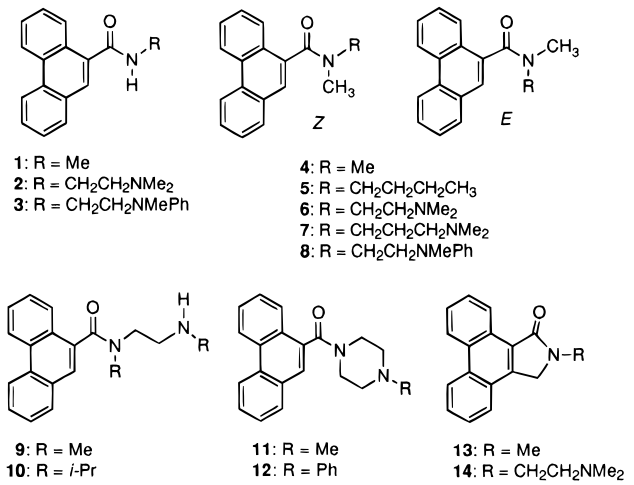

Results and Discussion

Synthesis and Structure of Linked Amides and Esters. The synthesis of the model amides **1** and **4** and lactam **13** have

[⊗] Abstract published in *Advance ACS Abstracts,* February 15, 1996.

0022-3654/96/20100-4055$12.00/0

previously been reported.[2,6] The linked amine−amides (**2**, **6**, **7**, and **9**−**11**) were prepared via the reaction of phenanthrene-9-carboxylic acid chloride with excess diamine. The aniline−amides (**3**, **8**, and **12**) were prepared by dicyclohexylcarbodiimide (DCC) coupling of phenanthrene-9-carboxylic acid with the appropriate diamine. The amine−lactam **14** was prepared via a modification of the synthesis of **13**. All products were purified by column chromatography followed by recrystallization and characterized by ^{1}H NMR, IR, absorption, and fluorescence spectral data. The crystal structure of **8** and solution conformational analysis of **5**−**8** will be reported elsewhere.[7]

The secondary amides **2** and **3**, piperazines **11** and **12**, and lactam **14** exhibit a single set of ^{1}H NMR resonances at room temperature for each type of proton. Thus, they exist either in a single conformation or in rapidly interconverting conformations. The chemical shifts of the aminoalkyl protons for **2** and **14** are similar, indicating that the secondary amide **2** exists in the *Z* conformation, as is normally the case for the secondary amides.[1] The piperazines **11** and **12** display separate signals for the amide α-methylene protons but a single amine *N*-methyl or *N*-phenyl signal.

Tertiary amides with inequivalent *N*-substituents usually exist as mixtures of *Z* and *E* conformers (Chart 1).[1] The spectra of **5**−**10** display two sets of resonances that can be assigned to the *E* and *Z* conformers on the basis of chemical shift data and solvent-induced shifts. α-Substituents *Z* to the carbonyl oxygen have larger chemical shifts than α-substituents *E* to the carbonyl, and *E* substituents display larger upfield shifts in benzene than *Z* substituents.[8] In the case of **9** and **10** these assignments were confirmed by spin-decoupling studies. The ratio of *E*/*Z* isomers for the tertiary amides can be determined by integration of the two *N*-methyl resonances (*N*-isopropyl in the case of **10**). The *Z* isomer content determined in this manner is 51−59% for **5**−**9** and 85% for **10**. The larger *Z* isomer content for **10** is consistent with the reported preference of bulky substituents for the *E* position in benzamides.[1,8] The *Z*/*E* ratios of **6**, **8**, and **10** are independent of temperature (−40 to 20 °C) in $CDCl_3$ solution and are also independent of solvent polarity.

The ground state conformations of the (aminoalkyl)amides **2**, **6**, and **11** were investigated using a modified MM2 force field as supplied in the *Chem 3D Plus* software package.[9] The phenanthrene−carbonyl dihedral angles (φ_1) were assumed to be the same as those calculated for the model compounds **1** and **4**. The potential energy surfaces for **1** and **4** are fairly flat for $50° < \varphi_1 < 120°$ with minima at 115° for **1** and 90° for **4** (relative to the planar s-cis enone conformation ($\varphi_1 = 0°$)). In the global minima for **2** and *Z*-**6**, the β-carbon of the aminoalkyl group is perpendicular to the amide plane and the amine and amide nitrogens are anti. The rotamer in which the nitrogens are gauche is calculated to be of slightly higher energy (1−2 kcal/mol). Minimized, folded conformations of *Z*-**6** and *E*-**6** are shown in Figure 1a. Overlap of the amine lone pair and phenanthrene π-orbitals is possible for the latter, but not the former, isomer. There are two global minima for **11** and **12**, corresponding to the two diastereomeric flattened piperazine chair conformers (Figure 1b). The twist boat is calculated to be higher in energy by ca. 5 kcal/mol. Thus, the two chair conformers are expected to interconvert rapidly at room temperature on the NMR time scale, in accord with the observation of a single set of proton resonances.

Absorption and Fluorescence Spectra. The electronic absorption and fluorescence spectra of the model compounds **1**, **4**, and **13** have been previously described.[2,6] All of the phenanthrene derivatives in the present study display two low-energy absorption bands similar in appearance to the ^1L_a and ^1L_b bands of phenanthrene and a more intense band at a shorter wavelength (ca. 225 nm). Absorption maxima and extinction coefficients in hexane solution are summarized in Table 1. The shorter wavelength maxima for lactams **13** and **14** are red-shifted with respect to those of the secondary and tertiary amides, presumably reflecting enhanced conjugation in the planar lactam vs nonplanar amides. Aminoalkyl substituents are observed to have only minimal effects on the position of the absorption maxima, indicating the absence of strong interaction between the phenanthrene and amine functional groups. Since the absorption maximum for *N*,*N*-dimethylaniline is at 298 nm (ϵ_A = 2200), an increase in the intensity of the short wavelength bands of **3**, **8**, and **12** was expected but not observed. We found no evidence for charge-transfer absorption bands such as those observed by Barlow et al.[10] for *N*-(aminoalkyl)phthalimides.

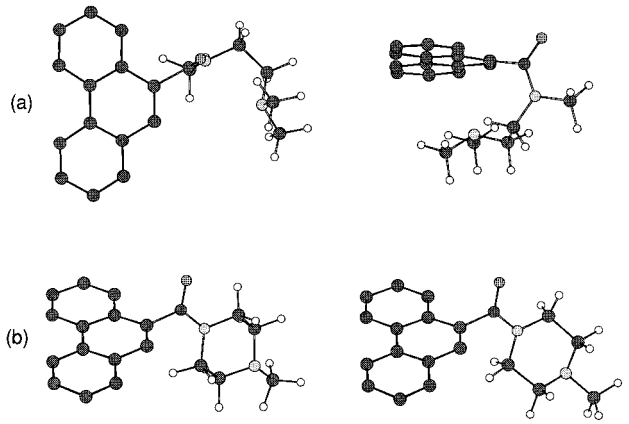

Figure 1. Folded conformations of (a) *Z*-**6** and *E*-**6** and (b) the two chair conformations of **12**.

TABLE 1: Absorption Maxima, Extinction Coefficients, and Fluorescence Maxima for Phenanthrene-9-carboxamides in Hexane Solution

amide	S_2, nm	ϵ_A ($M^{-1}cm^{-1}$)	S_1, nm	ϵ_A ($M^{-1}cm^{-1}$)	fl, nm
1	298	12900	350	180	372
2	299	11900	350	160	372
3	299	9370	350	130	372
4	298	10600	348	120	368
6	300	12700	348	130	368
7	300	9230	350	110	367
8	300	10600	349	130	366
9	300	11500	350	110	368
10	300	12700	350	210	368
11	298	11400	348	120	373
12	300	13900	350	150	375
13	316	9700	353	700	374
14					374

Room temperature fluorescence is observed for all of the phenanthrene derivatives investigated. Fluorescence maxima in hexane solution are reported in Table 1 and, like the long wavelength absorption maxima, display only minor variation with structure or solvent polarity. The fluorescence spectra of the tertiary amides and lactams (**4**−**13**) are highly structured, like the fluorescence of phenanthrene, whereas the fluorescence of the secondary amides **1**−**3** is broader. This difference is attributed to a change in geometry for the secondary amides (a decrease in φ_1, eq 1, in the singlet vs ground state) but not for the tertiary amides or lactams.[2] In addition to the locally excited fluorescence observed for all of the phenanthrene derivatives, structureless, long-wavelength emission attributed to intramolecular exciplexes (*vide infra*) is observed for the linked anilines **3** and **8**.

Fluorescence quantum yields (Φ_f), decay times (τ), and preexponentials (A) in hexane and acetonitrile solution are

TABLE 2: Fluorescence Quantum Yields and Lifetimes for Phenanthrene-9-carboxamides in Hexane and Acetonitrile Solution

	hexane		CH_3CN
amide	Φ_F	τ, ns[a]	τ, ns
1	0.09	23.7	27.4
2	0.04	14.1	5.3
3	<0.005	0.2	0.2
4	0.03	13.9	22.4
5	0.04	15.8	22.5
6-l	0.03	15.0 (0.69)	12.8 (0.27)
6-s		3.1 (0.31)	0.2 (0.79
7-l	0.03	14.7 (0.71)	18.5 (0.49)
7-s		8.7 (0.21)	1.2 (0.51)
8	<0.005	0.4, 0.40[b]	0.2, 0.22[b]
9-l	0.03	15.6 (0.65)	19.0 (0.055)
9-s		6.9 (0.35)	1.4 (0.45)
10-l	0.04	15.6 (0.73)	19.7 (0.75)
10-s	6.9 (0.27)	5.0 (0.25)	
11-l	0.01	5.3 (0.30)	8.8 (0.85)
11-s		3.8 (0.70)	5.0 (0.15)
12	<0.005	0.7	0.3
13	0.09	19.4	20.2
14	0.01	3.4	0.2

[a] Lifetime data determined with a time resolution of ca. 0.2 ns except as noted (preexponentials in parentheses). [b] Data obtained with a time resolution of 50 ps.

reported in Table 2. Decay profiles were obtained using a single photon counting apparatus, and the decays were deconvoluted using a single or multiple exponential least-squares analysis as described by James et al.[11a] Samples were excited near the maximum of the 255 nm absorption band and monitored near the emission maximum (Table 1). The time resolution of our apparatus is ca. 0.2 ns, and thus, decay times <0.5 ns should be regarded as approximate. The decay times for **8** are similar to those obtained using an apparatus with 50 ps time resolution. The decay times >1 ns reported as single exponentials in Table 2 are best fit by a single exponential decay ($A = 1.0$), and those reported as double exponentials are best fit as double exponentials. For decay times <1 ns, improved fits could be obtained with double or triple exponentials, but in all cases (including **3** and **8** for which exciplex fluorescence is observed) the reported decays account for >99% of the total locally excited fluorescence intensity and the goodness of fit, as judged by the randomness of residuals, autocorrelation function, and reduced χ^2 values < 1.2, was considered acceptable.

The secondary amides **1**−**3**, model tertiary amides **4** and **5**, and lactams **13** and **14** all display single exponential fluorescence decay. The tertiary amides display dual exponential fluorescence decay, except in the case of the aniline−amides **8** and **12**, which have decay times similar to the time resolution of our instrument. The decay times of **4**, **6**, and **11** were measured in several additional solvents (benzene, dichloromethane, and benzonitrile) and have values intermediate between those reported for hexane and acetonitrile.

The fluorescence lifetimes and quantum yields for the linked compounds are all shorter than those of the model compounds (Table 2). However, the fluorescence rate constants calculated from the measured lifetimes and quantum yields ($k_f = \Phi_f\tau^{-1}$) are similar for the linked compounds and the appropriate model compound. Thus, the shorter lifetimes of the linked compounds are attributed to the occurrence of intramolecular quenching rather than perturbation of the phenanthrene chromophore.

Inter- and Intramolecular Quenching. The fluorescence intensity (I) of the model compounds **1**, **4**, and **13** is quenched by added amines. Quenching of the fluorescence of **1**, **4**, and **13** by $PhNMe_2$ (but not by Et_3N or Et_2NH) is accompanied by the appearance of intermolecular exciplex fluorescence in nonpolar and moderately polar solvents. The slopes of linear Stern−Volmer plots (eq 2) for quenching by amine provide values of the quenching constant $k_q\tau$, where k_q is the rate constant for intermolecular quenching and τ is the singlet lifetime in the absence of quenching.[11b,c] Values of k_q calculated from the quenching constant and the measured singlet lifetime (Table 2) are reported in Table 3 along with the singlet energies and reduction potentials of the amides. The oxidation potentials of Et_2NH, Et_3N, and $PhNMe_2$ are 1.65, 1.42, and 1.16 V vs Ag/AgI.

TABLE 3: Energetics and Kinetics of Intermolecular Electron Transfer Quenching

		amide		
	solvent	**1**	**4**	**13**
E_S, eV[a]	hexane	3.42	3.52	3.56
E_A^{red}, V[b]	MeCN	−1.90	−2.04	−1.87
ΔG_{et}, eV (Et_3N)[c]	hexane	0.43	0.48	0.32
$10^{-9}k_{sv}$, M^{-1} s^{-1} (Et_3N)[d]	hexane	1.8	2.8	3.0
ΔG_{et}, eV (Et_3N)[c]	MeCN	−0.17	−0.12	−0.28
$10^{-9}k_{sv}$, M^{-1} s^{-1} (Et_3N)[d]	MeCN	5.4	2.6	4.7
ΔG_{et}, eV ($PhNMe_2$)[c]	hexane	0.18	0.22	0.07
$10^{-9}k_{sv}$, M^{-1} s^{-1} ($PhNMe_2$)[d]	hexane	2.3	1.7	1.2

[a] Singlet energy estimated from the highest energy fluorescence maximum. [b] Reduction potential vs Ag/AgI. [c] Calculated using eq 3. See text. [d] Rate constant for intermolecular quenching determined from the slope of linear Stern−Volmer plots (eq 2) and the measured lifetime (Table 3).

$$I^\circ/I = 1 + k_q\tau[\text{amine}] \qquad (2)$$

The observation of exciplex fluorescence upon quenching of **1**, **4**, and **13** by $PhNMe_2$ and the larger values of k_q for quenching by $PhNMe_2$ vs Et_3N are indicative of an electron transfer mechanism for fluorescence quenching. The free energy change for electron transfer quenching can be calculated from the singlet energies and redox potentials for the amides reported in Table 3 and the amine oxidation potentials using Weller's equation (eq 3), where C is an empirical solvent constant (0.54 eV in hexane and −0.06 eV) in acetonitrile).[12] The values of k_q for quenching by $PhNMe_2$ in hexane solution are near the rate of diffusion (ca. 2×10^{10} M^{-1} s^{-1}). The values of k_q for quenching by Et_2NH and Et_3N are smaller and display surprisingly little dependence on amide singlet state electron affinity ($E_A^{red} - E_S$), amine oxidation potential, or solvent polarity. Similar results were reported for quenching of *E*-stilbene and several arenes by secondary and tertiary aliphatic amines and attributed to the formation of an exciplex or heteroexcimer with only partial electron transfer character.[13] In such cases, exciplex formation is highly reversible and the rate constant k_q is determined by the rates of exciplex formation, dissociation, and decay.[11b,c]

$$\Delta G_{et} = E_D^{ox} - E_A^{red} - E_S + C \qquad (3)$$

The linked amine−amides **2** and **3** and amine−lactam **14** display single exponential decay with fluorescence quantum yields and lifetimes smaller than those of the model compounds **1** and **13** (Table 2). Since the values of k_f for the linked amines are similar to those for the model compounds, we assume that the decrease in lifetime is a consequence of intramolecular electron transfer quenching. Rate constants for intramolecular quenching (k_q) calculated from the lifetimes of the linked amine (τ) and model compound (τ_0) using eq 4 are reported in Table 4. Intramolecular photoinduced electron transfer between arenes and amines separated by a flexible polymethylene chain has

TABLE 4: Calculated Rate Constants for Intramolecular Quenching[a]

amide	$10^{-6}k_q$, M^{-1} (hexane)	$10^{-6}k_q$, M^{-1} (MeCN)
2	29	150
3	4900	>5000
Z-**6**	3.4	34
E-**6**	260	>5000
Z-**7**	4.7	9.6
E-**7**	52	790
8	2400	4500
Z-**9**	0.8	8.2
E-**9**	82	670
Z-**10**	0.8	6.3
E-**10**	82	160
11	130200	69160
12	1400	3300
14	260	>5000

[a] Values calculated using eq 4 and lifetime data from Table 3.

been extensively investigated.[14] In nonpolar solvents, arene−trialkylamine exciplexes are proposed to adopt specific folded conformations that maximize orbital overlap and Coulombic attraction while avoiding high-energy conformations of the polymethylene chain. The relatively slow values of k_q for intramolecular quenching by *N*,*N*-dimethylamines **2** and **14** may reflect conformational restrictions on overlap between the arene and amine as well as the endergonic nature of electron transfer.

$$k_q = \tau^{-1} - \tau^{\circ -1} \tag{4}$$

Dual exponential fluorescence decay is observed for all the flexibly linked amine−tertiary amides **6**−**10** except **8** (Table 3). The lifetimes of both components are shorter than those of the model tertiary amides **4** and **5**. The two decays are assigned to the *E* and *Z* conformers based on the reasonable assumption that interconversion of these conformers is slow on the time scale of fluorescence decay.[15] The observation of dual exponential decay requires the presence of a covalently attached amine quencher, as evidenced by the observation of single exponential decay from the model amide **5**, which exists as a 1:1 mixture of *E* and *Z* conformers. The rate constants for intramolecular quenching by the two conformers can be calculated using eq 4 and the measured lifetimes. The assignment of the larger values of k_q to the *E* isomers is based upon the anticipated differences in phenanthrene−amine orbital overlap in the *E* vs *Z* isomer (Figure 1a). This assignment is supported by the effects of replacing the amide *N*-methyl of **9** with the *N*-isopropyl of **10**, which results in an increase in the ground state population of the *Z* conformer and an increase in the preexponential for the longer-lived fluorescence decay (Table 2).

A related example of isomer-dependent intramolecular electron transfer quenching has recently been reported by de Silva et al.[16] The observation of efficient intramolecular electron transfer quenching for the naphthalimide **15**, but not for **16**, was attributed to the intramolecular charge-transfer character of the naphthalimide singlet state. The flexibly linked amine in **15** can directly overlap the electron-deficient region of the singlet state, whereas the linked amine in **16** is connected to the electron-rich region of the singlet state.

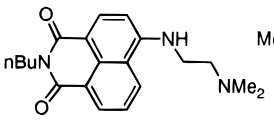

15

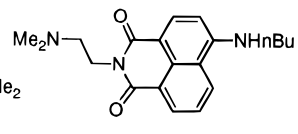

16

The values of k_q assigned to the *Z* isomers of the (*N*,*N*-dimethylamino)ethylamides increase in the order *Z*-**6** < **2** < **14** (Table 4). The structure dependence of intramolecular quenching stands in marked contrast to intermolecular quenching, which is essentially independent of the amide structure or amine oxidation potential (Table 3). One possible reason for this difference is that overlap of the singlet phenanthrene and amine orbitals is possible for intermolecular quenching but not for intramolecular quenching of the *Z* isomers. The amide group serves as an intermediary in the intramolecular quenching of singlet phenanthrene by the aminoalkyl group. Interaction of the phenanthrene and amide π-orbitals should be most effective when these groups are coplanar, as in the lactams **13** and **14**.[17] The planar lactam **13** also has a lower reduction potential than the tertiary amide **4** (Table 3). Thus, the increase in rate constant for *Z*-**6** < **2** < **14** may reflect a decrease in the dihedral angle φ_1 (eq 1) in this series of molecules.

Changing the aminoalkyl linker from ethyl to propyl in **6** vs **7** has little effect on the k_q values of the *Z* isomer but results in a decrease in k_q for the *E* isomer (Table 4). The extended linker in *Z*-**7** still does not permit direct phenanthrene−amine orbital overlap. The extended linker in *E*-**7** is expected to increase the entropic requirement for intramolecular exciplex formation without improving the orbital overlap, resulting in a decrease in k_q. Changing the quencher from a tertiary amine to a secondary amine in **6** vs **9** or **10** results in a decrease in k_q for both *Z* and *E* isomers, providing another instance of greater structural sensitivity for intra- vs intermolecular quenching. Secondary amines are expected to be much poorer quenchers than tertiary amines on the basis of their higher oxidation potentials. However, N−H−arene hydrogen bonding may help stabilize secondary amine exciplexes.[13b] Such hydrogen bonding is not possible for the *Z* isomers of the (aminoalkyl)amides.

The *N*-methylpiperazine **11** provides an interesting example of dual exponential decay in a molecule with a semirigid linker.[18] We tentatively assign the two fluorescence decays (Table 2) to the two diastereomeric chair conformations, which have similar MM2-minimized energies (Figure 1b). The barrier for ring inversion of piperazines is too small to permit observation of the two diasteromers by NMR but should be large enough to prevent singlet state equilibration. Both of the values of k_q for **11** are more similar to those for the *E* vs *Z* isomers of **6** and **7**, even though phenanthrene−amine orbital overlap is not possible for **11**. The larger values of k_q for **11** vs *Z*-**6** might reflect either a lower amine oxidation potential[19] or involvement of through-bond interactions in the quenching process. Brouwer et al.[20a] have observed extensive through-bond interaction in the cation radical of *N*,*N*′-dimethylpiperazine.

Single exponential decay is observed for the aniline−amides **8** and **12** (Table 2), even though the former exists as a mixture of *Z* and *E* isomers and the latter as a mixture of chair conformers. The observed fluorescence decay constants are near the time resolution of our instrumentation. Hence, a more rapid decay would not be resolved from the lamp profile and two similar decay constants most likely would not be resolved. Assuming the observed decay for **8** is that of the *Z* isomer, the calculated quenching rate constant for Z-**8** is 700 times that of Z-**6** (Table 4). This large rate enhancement can be attributed to the lower ionization potential and smaller nuclear reorganization energy for oxidation of the aromatic vs aliphatic amines. π-Donors such as aniline are also reported to be more effective long-range donors than are n-donors such as trialkylamines.[20b]

Solvent Dependence of Electron Transfer Quenching. Rate constants for intermolecular quenching of **1**, **4**, and **13** by

TABLE 5: Exciplex Fluorescence Maxima and Decay Times

exciplex	solvent	λ_{max}, nm	τ_{ex}, ns[a]
1:$PhNMe_2$	hexane	467	
	diethyl ether	489	
	dichloromethane	512	
3	hexane	450	0.6 (0.51), 2.0 (0.49)
	THF	525	0.8 (0.69), 2.5 (0.31)
			0.6 (0.61), 2.3 (0.38)[b]
	MeCN[c]	560	
4:$PhNMe_2$	hexane	440	2.8
	diethyl ether	469	5.4
	dichloromethane	495	3.2
8	hexane[c]	418	
	THF	470	0.6 (0.69), 3.5 (0.31)
	MeCN	510	0.2 (0.68) , 1.2 (0.32)

[a] Decay times in nitrogen-purged solutions determined at emission maximum except as noted. Values in parentheses are decay preexponentials. [b] Decays monitored at 450 nm. [c] Very weak exciplex fluorescence.

$PhNMe_2$ are near the diffusion limit in hexane solution (Table 3) and have similar values in acetonitrile solution. Singlet decay times for the linked anilines **3**, **8**, and **12** are near the time resolution of our instrumentation in hexane and are even shorter in acetonitrile (Table 2). Rate constants for intermolecular quenching of **1**, **4**, and **13** by Et_3N are approximately a factor of 10 below the diffusion limit in hexane solution and show small, variable increases in acetonitrile solution (Table 3). The small solvent effect, like the weak dependence on ΔG_{et}, is consistent with a relatively small extent of electron transfer in the quenching process. The solvent dependence of the value of k_q for intramolecular quenching by linked *N*,*N*-dimethylalkylamines displays an interesting structural dependence. Most of the *Z* isomers (**2**, **6**, **9**, and **14**) and *E* isomers (**6**, **7**, and **9**) display moderate rate increases (factors of 5 to 20) in acetonitrile vs hexane solution (Table 4). Smaller increases in k_q are observed for *Z*- and *E*-**10**, plausibly reflecting steric hindrance of solvation of the bulky isopropyl amine.

In the case of the piperazine **11**, a decrease in k_q is observed in acetonitrile vs hexane solution. A decrease in the value of k_q as the solvent dielectric increases beyond ca. 20 is fairly common for rigidly linked donor−acceptor systems.[3b,21] This behavior has been explained in terms of Marcus theory as resulting from a greater increase in the solvent reorganization energy relative to ΔG_{ET} as the solvent dielectric constant increases. In physical terms, at the transition state a charge is produced before solvent reorganization can occur. The solvent shell initially corresponds to a neutral molecule and thus will be destabilizing to the charged state. This solvent-induced barrier increases as the solvent dielectric constant increases, resulting in a decrease in the probability of charge transfer and in the observed value of k_q. Systems with flexible linkers can adopt folded conformations, decreasing their dipole moments and thus reducing the solvent-induced barrier.

Exciplex Fluorescence. As previously noted, intermolecular fluorescence quenching of **1** and **4** by *N*,*N*-dimethylaniline is accompanied by the appearance of exciplex fluorescence. Exciplex fluorescence is also observed upon intramolecular fluorescence quenching in the aniline−amides **3** and **8** but not **12**. Exciplex fluorescence maxima in several solvents are reported in Table 5. The maxima for the secondary amide exciplexes (**1**:aniline and **3**) are at lower energy than those for the tertiary amide exciplexes (**4**:aniline and **8**) in hexane solution the difference in energy being comparable to the difference in reduction potentials for **1** vs **4** (Table 3). The exciplex fluorescence intensity for **8** is very weak in hexane and stronger in more polar solvents, including acetonitrile, whereas the exciplex fluorescence intensities of **1**:aniline, **3**, and **4**:aniline are strong in hexane and very weak in acetonitrile.

The observation of fluorescence from aniline−amide exciplexes, but not from trialkylamine−amide exciplexes, is analogous to the behavior reported by Barlow et al.[10] for the *N*-(aminoalkyl)phthalimides **17** and **18**. The lower oxidation potential of anilines vs trialkylamines should result in the formation of more stable exciplexes (eq 3). In addition, the Franck−Condon factor for exciplex fluorescence may be unfavorable for trialkylamine exciplexes because of the large change in geometry between the pyramidal neutral and planar cation radical.[14a] Intramolecular exciplex fluorescence has been observed for the linked (aminoalkyl)phenanthrenes **19**−**21**, even though the thermodynamics of electron transfer are even less favorable than for the amine−amides investigated in this study.[22,23] In the case of **19** exciplex fluorescence is observed in hexane,[22] whereas moderately polar solvents are necessary for the observation of exciplex fluorescence from **20** and **21**.[23] The differences in linked (aminoalkyl)phenanthrenes can be correlated to geometric restrictions upon overlap of the phenanthrene and amine. Overlap requires little nuclear motion in the case of **19**, chain folding in the case of **20** or **21**, and is geometrically impossible in the case of **2** or the *Z* isomers of **6** and **7**.

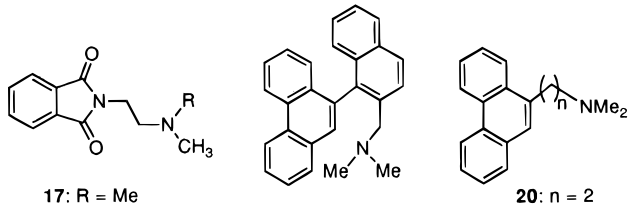

17: R = Me
18: R = Ph

19

20: n = 2
21: n = 3

Exciplex fluorescence is observed for the aniline−amide **3** even though the aminoalkyl group is *Z* with respect to the amide carbonyl and thus cannot achieve direct overlap with the phenanthrene π-orbitals. Arene−aniline exciplexes adopt a sandwich-type geometry when possible. However, exciplex fluorescence has been observed for intramolecular arene−aniline exciplexes that cannot adopt sandwich geometries.[24] The absence of exciplex fluorescence from the piperazine **12** indicates that some conformational mobility is required for exciplex formation, even in the case of the stronger aniline donors. We presume that the fluorescent exciplex of **3** has a folded geometry similar to that shown for Z-**6** in Figure 1a. In this geometry there is no direct overlap of phenanthrene (acceptor) and amine (donor) orbitals and the amide acts as an intermediary in the electron transfer process.

Since **8** exists as a mixture of *Z* and *E* isomers (1.3:1 ratio), its exciplex fluorescence (Table 5) might be attributed to either one or both of these isomers. Similarities between the behavior of the exciplexes formed by **3** and **8** suggest that the exciplex fluorescence of **8** arises only from the *Z* isomer. The slopes of Lippert−Mataga plots[26] (Figure 2) of the exciplex energy vs the solvent polarity parameter Δf (eqs 5 and 6) are similar for **3** and **8**. The slopes of the plots for the intramolecular exciplexes are larger than those for the intermolecular exciplexes. This difference in slopes is indicative of a larger exciplex dipole moment for the intra- vs intermolecular exciplexes, which could result from a larger separation of arene acceptor and amine donor in the intramolecular exciplex. The identical slopes of the Lippert−Mataga plots for **3** and **8** indicate that they most likely have similar geometries. The more compact, folded geometry expected from *E*-**8** should have a

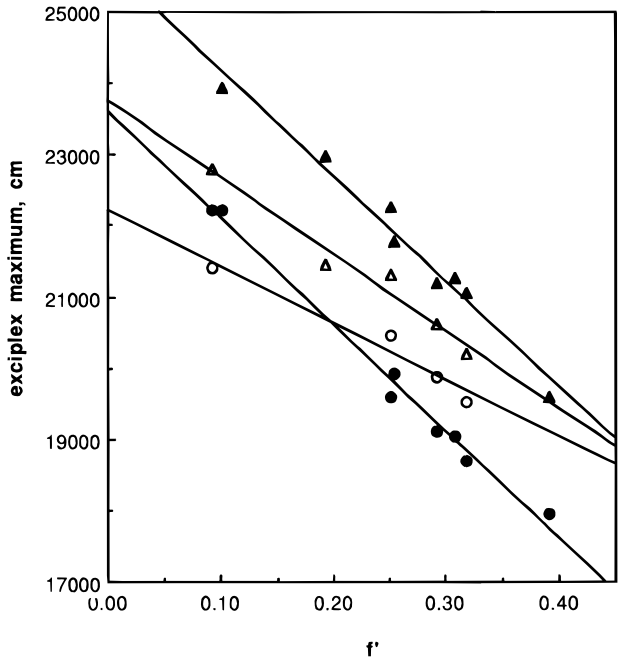

Figure 2. Solvent polarity dependence of the exciplex fluorescence maxima for **1**:PhNMe$_2$ (○), **3** (●), **4**:PhNMe$_2$ (△), and **8** (▲).

dipole moment similar to that of the intermolecular exciplexes and smaller than that of **3**.

$$\nu_{ex} = \nu_{ex}^{\circ} - (2\mu^2/hc\rho^3)\Delta f \quad (5)$$

$$\Delta f = (\epsilon - 1)/(2\epsilon + 1) - (n^2 - 1)/(4n^2 + 2) \quad (6)$$

Our assignment of the exciplex fluorescence from **8** to the *Z* isomer leaves to be answered the question of why the exciplexes of *E*-**6**−**8** are nonfluorescent even though electron transfer quenching is rapid and arene−amine orbital overlap can readily be achieved. The absence of exciplex fluorescence from an intramolecular exciplex in nonpolar solvents requires that return electron transfer and/or intersystem crossing be very rapid. As discussed in the following section, the observation of phosphorescence from *E*-**8** in low-temperature glasses suggests that rapid intersystem crossing may be responsible for the absence of exciplex fluorescence from *E*-**8**.

Single exponential exciplex decay is observed for the intermolecular exciplex **4**:PhNMe$_2$, whereas more complex decay is observed for the intramolecular exciplexes (Table 5). The exciplex decays reported for **3** and **8** were obtained from triexponential fits ($\chi^2 < 1.25$) in which the two reported components account for >99% of the fluorescence intensity. Both of the reported exciplex decay times are longer than the locally excited fluorescence decays reported in Table 2, indicating that exciplex formation is largely irreversible. Our inability to detect a rising component in the exciplex decays is consistent with locally excited decay times, which are comparable to the time resolution of our apparatus. In the case of **3** the two exciplex decays at different emission wavelengths in THF solution have slightly different preexponentials.

One possible explanation for the observation of dual exponential exciplex decay with similar contributions to the total fluorescence intensity for **3** and **8** (Table 5) is that there are two noninterconverting exciplex geometries. A similar explanation for dual exponential exciplex decay has been proposed by Helsen et al.[25] for some intramolecular pyrene−indole exciplexes. Two exciplex geometries could result from folding of the aminoalkyl group over the nonequivalent faces of the amide

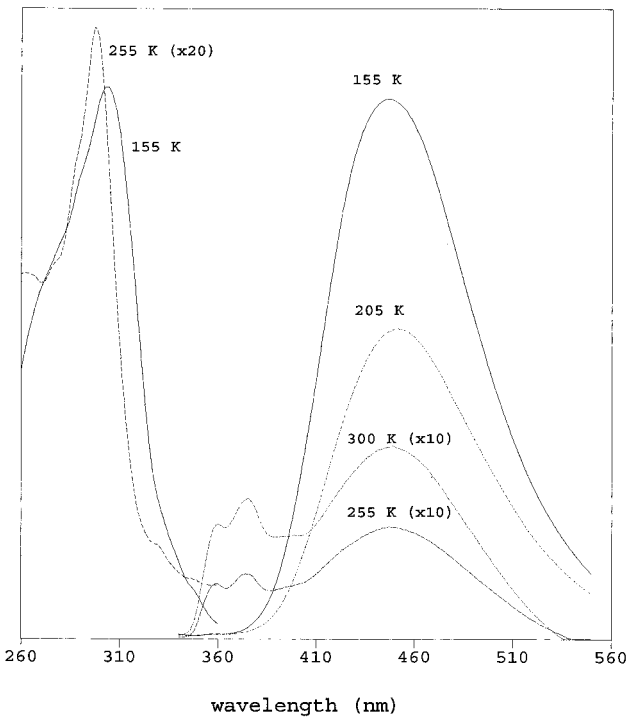

Figure 3. Temperature dependence of the fluorescence excitation and emission spectra of **3** in methylcyclohexane solution.

group. In order to test this possibility, the fluorescence behavior of the corresponding 9-anthracenecarboxamide **22** was investigated. Dual exponential intramolecular exciplex decay was observed for **22** even though the two amide faces are equivalent. Two exciplex geometries could also result from folding of the aminoalkyl group over the amide with either the *N*-phenyl or the *N*-methyl occupying the position cis to the carbonyl oxygen in the folded conformation.

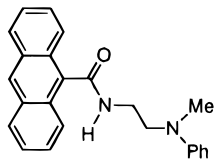

22

Temperature Dependence of Exciplex Fluorescence. The temperature dependence of the fluorescence excitation and emission spectra of the linked aniline−amides **3** in methylcyclohexane (MC) solution are shown in Figure 3. Decreasing temperature results in a marked increase in exciplex fluorescence intensity at temperatures below 250 K. Similar behavior is observed for **8**. There is little change in the appearance of the excitation or emission spectra of **3** or **8** below the glass transition temperature of MC other than the appearance of phenanthrene-like phosphorescence (λ_{max} = 470 nm) from **8**. Phosphorescence is also observed for the piperazine **12** at 77 K in a MC glass. Weak, structureless emission ($\lambda_{max} \sim$ 420 nm) is also observed from **12** in the glass but not in fluid solution at or above 155 K. To summarize, at 77 K we observe only exciplex fluorescence from **3**, which exists exclusively in the *Z* configuration, a mixture of exciplex fluorescence and locally excited phosphorescence from **8**, which exists as a mixture of *E* and *Z* isomers, and mainly phosphorescence from **12**. These observations support the proposal that only *Z* isomers form fluorescent exciplexes.

The increase in exciplex fluorescence intensity with decreasing temperature for **3** and **8** is accompanied by a change in the

dominant decay from the short-lived components observed at room temperature (Table 5) to long-lived components at 205 K and below. At 155 K the decay of **3** is dominated by two components with decay times of 16 and 52 ns and the decay of **8** by components with decay times of 22 and 66 ns. Weakly bound intramolecular arene−amine exciplexes often display a modest increase in exciplex fluorescence intensity and lifetime with decreasing temperature as a consequence of enhanced through-bond interactions[14a] or decreased rate constants for exciplex dissociation.[23,27] However, intramolecular exciplex fluorescence usually is very weak below the glass transition temperature because of restricted conformational mobility. Exceptions to this generalization have been reported. Okada and Mataga[28] observed a high ratio of exciplex:locally excited fluorescence for the linked (aminoalkyl)anthracene **23** and suggest that a loosely bound "molecular pair" might be formed in the matrix. Barlow et al.[10] also observed exciplex fluorescence from **18** at 77 K in several glassy matrices. The ratio of exciplex:locally excited fluorescence intensity was found to increase with increasing concentration in an ethanol glass, leading to the proposal that exciplex fluorescence might be attributed to molecular aggregates.

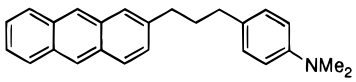

2 3

Several lines of evidence support the assignment of the intense, long-lived exciplex fluorescence observed for **3** and *Z*-**8** below 250 K (Figure 3) to molecular aggregates. Among these are the increase in the exciplex fluorescence intensity and broadening of the fluorescence excitation spectra at low temperatures and the similar appearance of the total emission spectrum above and below the glass transition temperature. Moreover, increasing the concentration of **3** from 10^{-5} to 10^{-4} M has little effect on the ratio of exciplex:locally excited fluorescence at 295 K or in the 77 K glass but results in an increase in this ratio from 4:1 to 12:1 at 205 K. Both **3** and *Z*-**8** can pack as head-to-tail dimers (or extended aggregates), whereas the geometrical constraints of the piperazine ring prevent **12** from forming head-to-tail dimers. The geometry of the intermolecular phenanthrene−aniline ground state complex is presumably similar to that for the van der Waals complexes of anthracene with anilines.[29] Folded ground state conformers have been implicated in some intramolecular electron transfer processes and exciplex formation and might be responsible, in part, for the strong low-temperature exciplex emission for **3** and **8**.[30]

Conclusion

The ease of construction of the amide linkage has permitted the investigation of intramolecular electron transfer for a large number of aminoalkyl-9-phenanthrenecarboxamides. Tertiary (aminoalkyl)amides **6**−**10** exist as mixtures of *Z* and *E* conformers in which the planar amide group is essentially orthogonal to the phenanthrene plane in solution. The piperazines **11** and **12** exist as mixtures of chair conformers. Secondary (aminoalkyl)amides exist predominantly as *Z* conformers and have smaller excited state phenanthrene−amide dihedral angles, whereas the lactam ring in **14** is planar.

These conformational properties have a pronounced effect upon the intramolecular electron transfer quenching of amide-linked phenanthrene−amines. More rapid quenching is observed for the *E* vs *Z* conformers of the tertiary amides as a consequence of more effective overlap of the phenanthrene (acceptor) and amine (donor) orbitals (Figure 1a). Rate constants for quenching by *Z* conformers increase as the phenanthrene−amide dihedral angle φ_1 (eq 1) decreases, owing to increased mixing of the arene and amide frontier orbitals. Dual exponential decay observed for the piperazines **11** and **12** is attributed to slightly different rates of intramolecular electron transfer in the two chair conformers (Figure 1b). Increasing solvent polarity results in an increase in the rates of intramolecular electron transfer for the flexible (aminoalkyl)amides but a decrease in rates for the semirigid piperazines. Intramolecular quenching is far more sensitive than intermolecular quenching to changes in the solvent, the phenanthrene singlet state reduction potential, and the amine oxidation potential.

Exciplex fluorescence is only observed for the *Z* conformers of aniline donors. A pronounced increase in exciplex fluorescence intensity and lifetime is observed below 250 K in methylcyclohexane solution or the frozen glass. These changes are attributed to the formation of ground state dimers or aggregates at low temperatures. The exciplexes of *E* conformers apparently decay via intersystem crossing. The less stable exciplexes formed by the *Z* and *E* conformers of trialkylamine donors are nonfluorescent.

The aminoalkyl-9-phenanthrenecarboxamides are moderately stable upon exposure to ultraviolet light in deoxygenated solution. Intramolecular arene−amine photoaddition reactions have been observed for secondary, but not tertiary, (aminoalkyl)-phenanthrenes.[22,23] Intramolecular cycloaddition reactions have also been observed for ester-linked styrene−phenanthrenecarboxylates.[31] The photostability of the (aminoalkyl)phenanthrenes plausibly reflects the short lifetimes of the exciplex intermediates or the absence of least-motion pathways for exciplex proton transfer processes.[14g,h]

Experimental Section

General Methods. Melting points were determined on a Fisher-Johns apparatus and are uncorrected. ^{1}H NMR spectra were recorded on a Varian Gemini 300 or Varian XLA 400 spectrometer with TMS as an internal standard. UV−visible absorption spectra were measured with a Hewlett-Packard 8452 A diode-array spectrometer. Fluorescence spectra were recorded using a Spex Fluoromax. Samples of 10^{-5} M phenanthrene derivative in dried solvent contained in a square quartz cell equipped with a side arm and serum cap were deoxygenated by purging with nitrogen for 10 min. For low-temperature fluorescence spectra, a nitrogen-cooled Oxford Instruments optical cryostat (DN 1704) connected to an ITC 4 temperature controller (±0.5 K) was mounted in the sample compartment of the fluorescence spectrophotometer. IR spectra were recorded using a Mattson FT-IR. Fluorescence quantum yields were determined relative to phenanthrene in hexane ($\Phi_F = 0.13$)[32] for solutions of matched absorbance (ca. 0.1 OD).

Fluorescence decays were acquired for solutions prepared as described above using a PTI-LS1 single photon counting instrument with a gated hydrogen arc lamp (time resolution ca. 0.2 ns). Samples were excited at 260 nm ($A \sim 0.5$) and decays measured at the emission maximum with the acquisition of 12 000 counts in the peak channel. The decays were deconvoluted using a single or multiexponential least-squares analysis as described by James et al.[11a] The goodness of the fit was judged by the reduced χ^2 value as well as the randomness of the residuals and the autocorrelation function. The χ^2 values were less than 1.2.

Cyclic voltammetric experiments were performed with a three-electrode Bioanalytical Systems Inc. (BAS) apparatus in nitrogen-purged acetonitrile solutions using Et_4NBF_4 as the

electrolyte.[33] The reference electrode consisted of Ag/AgI separated from the solution by a fitted glass bridge with a VYCOR membrane and filled with a saturated Et_4NI solution in CH_3CN. The working electrode (BAS) consisted of a 1.5 mm diameter polished platinum disk embedded in a cobalt glass seal. The counterelectrode was a platinum wire (BAS). The scan rate was 0.10 Vs^{-1} and the step size was 2.44 mV. The halfwave potential of ferrocene was 0.668 ± 0.005 V under these conditions.

The force-field-type calculations were performed on a Macintosh IIsi computer using an MM2-type field as supplied in the *Chem 3D* software package.[9]

A series of alkyl-chain conformations were examined. All bonds and angles were allowed to relax to a minimum convergent energy on the force field surface for a range of linker conformations to determine local and global energy minima. In most cases this was done for more than one very similar geometry to ensure a true local minimum.

Materials. Dichloromethane (Aldrich) was distilled over calcium hydride prior to use. Benzene (Aldrich) was distilled over sodium metal prior to use. Tetrahydrofuran (Aldrich) was distilled over molecular sieves prior to use. All other solvents were freshly opened spectral grade or HPLC grade (Aldrich and Fisher) and were used without further purification. Diethylamine (Aldrich) and triethylamine (Aldrich) were distilled prior to use. *N*-methylaniline (Aldrich) and *N*,*N*-dimethylaniline-(Aldrich) were distilled under reduced pressure prior to use. *N*,*N*-dimethylethylenediamine, *N*,*N*,*N*′-trimethylethylenediamine, *N*,*N*′-dimethylethylenediamine, *N*,*N*′-diisopropylethylenediamine, *N*,*N*,*N*′-trimethylpropylenediamine, *N*-methylpiperizine, *N*-phenylpiperizine, *N*-methyl-*N*-isopropylamine, and *N*,*N*-dimethylethylamine (Aldrich) were used as received. The synthesis of phenanthrene-9-carboxylic acid chloride, **1**, **4**, and **13** have been previously described.[2,6]

N-Methyl-N-phenylethylenediamine. *N*-methylaniline (0.09 mol) and sodium methoxide (Aldrich, 0.095 mol) were mixed in methanol (50 mL) and cooled to 0 °C in an ice bath. To this mixture, α-bromoethylacetate (Aldrich, 0.09 moles) was added by addition funnel over 1 h while stirring. After addition was completed, the mixture was stirred 2 more hours at 0 °C and then overnight at room temperature. The solvent was removed under vacuum and the residual oil dissolved in ethyl ether (50 mL). The organic layer was washed with 5% aqueous NaOH and then H_2O. The organic layer was dried with $CaCl_2$ and the solvent removed. TLC ($CHCl_3$/MeOH, 3/2) showed one product. The crude 2-(*N*-methylaniline)ethylacetate (0.09 mol) and sodium methoxide (0.095 mol) were dissolved in methanol (50 mL) and bubbled with ammonia (Fluka) for 15 min. The mixture was sealed and stirred overnight at 40 °C and then refluxed for 8 h. The solvent was removed under vacuum and the residual oil dissolved in ethylacetate, washed with 5% aqueous NaOH and then with H_2O. The organic layer was dried with $CaCl_2$ and the solvent removed. The crude solid was dissolved in hot ethylacetate and cooled to yield 4 g (27%) of 2-(*N*-methylaniline)acetamide as gray plates. mp 168−9 °C. ^{1}H NMR ($CDCl_3$): d = 3.04 (s, 3H), 3.87 (s, 2H), 5.53 (b, 1H), 6.46 (b, 1H), 6.76 (d, 2H), 6.85 (t, 1H), 7.27 (t, 2H).

The 2-(*N*-methylaniline)acetamide (0.011 mol) was dissolved in tetrahydrofuran (25 mL) and slowly added to a stirred mixture of $LiAlH_4$ (0.044 mol) in refluxing tetrahydrofuran (50 mL). The mixture was refluxed for 48 h. After cooling, the excess $LiAlH_4$ was reacted with H_2O (ca. 2 mL), the solution was filtered, dried with $CaCl_2$, and the solvent removed to yield a 1.6 g of *N*-methyl-*N*-phenylethylenediamine as a brown oil (100%, 27% overall). ^{1}H NMR ($CDCl_3$): d = 2.90 (t, 2H), 2.94 (s, 3H), 3.37 (t, 2H), 6.70 (t, 1H), 6.75 (d, 2H), 7.22 (t, 2H).

TABLE 6: Synthesis and Characterization of 9-Phenanthrenecarboxamides

compound	method, yield	mp (°C)	IR (C=O, cm^{-1})	^{1}H NMR amide Me	^{1}H NMR amine Me
2	A, 79%	124−5	1651.2		2.27
3	B, 7%	178−9	1658.9		3.02
5	A, 81%	oil	1620.3	2.83, 3.25[a]	
6	A, 16%	oil	1624.2	2.87, 3.29[a]	2.41, 1.90[a]
7	A, 54%	oil	1624.2	2.85, 3.27[a]	2.32, 1.98[a]
8	B, 11%	143−4	1628.0	3.10, 3.35[a]	2.84, 2.64[a]
9	A, 89%	76−9	1624.2	2.88, 3.28[a]	2.59, 2.14[a]
10	A, 34%	oil	1614.5	1.11, 1.43[b]	1.30, 0.69[b]
11	A, 75%	102−4	1616.5	3.29, 4.0[d]	2.32
12	B, 9%	188−9	1630.0	3.43, 4.1[d]	
14	C, 4%	144−6	1672.4	4.85[e]	2.35

[a] Chemical shifts (ppm) in $CDCl_3$ solution. First value is for the *Z* isomer, and the second is for the *E* isomer. [b] Chemical shift of isopropyl methyl group. First value is for the *Z* isomer. [d] Chemical shifts of α-methylenes. [e] Chemical shift of lactam methylene.

N,N′-Dimethyl-N-phenylethylenediamine. *N*,*N*′-dimethyl-*N*-phenylethylenediamine was synthesized in an analogous manner using methylamine gas (Fluka). *N*-methyl-2-(*N*′-methylaniline)-acetamide was isolated as a yellow solid (41%). ^{1}H NMR ($CDCl_3$): d = 2.84 (d, 3H), 3.01 (s, 3H), 3.86 (s, 2H), 6.60 (b, 1H), 6.73 (d, 2H), 6.85 (t, 1H), 7.28 (t, 2H). *N*,*N*′-dimethyl-*N*-phenylethylenediamine was isolated as a brown oil (40% overall). ^{1}H NMR ($CDCl_3$): d = 2.29 (s, 2H), 2.47 (s and t, 2H), 2.81 (t, 1H), 2.95 (s, 3H), 3.46 (m, 2H), 6.70 (t, 1H), 6.77 (d, 2H), 7.23 (t, 2H).

The phenanthrene-9-carboxamide derivatives were synthesized by the three general methods described below. The method, yield, mp, and IR and ^{1}H NMR data are summarized in Table 6. Absorption and fluorescence spectral data are summarized in Table 1.

Method A.[34] Phenanthrene-9-carboxylic acid chloride (0.0025 mol) was dissolved in benzene (5 mL), and an excess of the amine (ca. 10 equiv) was added. The mixture was stirred overnight at 35 °C. The solution was dissolved in ethylacetate (50 mL) and washed 2 times with 5% aqueous HCl (50 mL), 2 times with 5% aqueous KOH (50 mL), and 2 times with H_2O. The organic layer was dried with $CaCl_2$ and the solvent removed under vacuum. The product was then purified by column chromatography (silica, $CHCl_3$, or $CHCl_3$/5%MeOH), and solid products were recrystallized 2 times from either ethylacetate, ethylacetate/ hexane, or EtOH.

Method B.[35] This method was used for the aniline derivatives that were not stable in the presence of the acid chloride. Phenanthrene-9-carboxylic acid (0.0045 mol) was mixed with the amine (0.006 mol) and 1,3-dicyclohexylcarbodiimide (DCC, Aldrich, 0.005 mol) in benzene (30 mL) under N_2. The mixture was stirred overnight at room temperature. The solvent was evaporated and the DCC salt was removed by successive suspension of the crude mixture in ethyl ether and filtration. The product was then purified by column chromatography (silica, $CHCl_3$) 2 times and then recrystallized 2 times from ethylacetate/hexane.

Method C.[6] The lactam **14** was prepared by the method employed for the preparation of **13** using *N*,*N*-dimethylethlenediamine instead of methylamine.

Acknowledgment. Financial support for this project was provided by the National Science Foundation. We thank F. G. Bordwell for the use of the electrochemical equipment, M. Gahr

for the subnanosecond lifetime measurements, A. M. Miller for some of the steady state absorption and fluorescence data, and B. A. Yoon for some of the NMR spectral data.

References and Notes

(1) Stewart, W. E.; Siddall, J. H. *Chem. Rev.* **1970**, *70*, 517.

(2) Lewis, F. D.; Barancyk, S. V.; Burch, E. L. *J. Am. Chem Soc.* **1992**, *114*, 3866.

(3) (a) Schmidt, J. A.; McIntosh, A. R.; Weedon, A. C.; Bolton, J. R.; Connolly, J. S.; Hurley, J. K.; Wasielewski, M. R. *J. Am. Chem Soc.* **1988**, *110*, 1733. (b) Liu, J. Y.; Bolton, J. R. *J. Phys. Chem.* **1991**, *95*, 6924.

(4) Wasielewski, M. R. *Chem. Rev.* **1992**, *92*, 435.

(5) For a preliminary account of this aspect of our results see the following. Lewis, F. D.; Barancyk, S. V.; Burch, E. L. *J. Am. Chem Soc.* **1994**, *116*, 1159.

(6) Lewis, F. D.; Burch, E. L. *J. Photochem. Photobiol. A*, in press.

(7) Lewis, F. D.; Burch, E. L. Manuscript in preparation.

(8) Lewin, A. H.; Frucht, M. *Org. Magn. Reson.* **1975**, *7*, 206.

(9) *Chem3D Plus*; Cambridge Scientific Computing, Inc.: Cambridge, MA, 1990.

(10) Barlow, J. H.; Davidson, R. S.; Lewis, A.; Russell, D. R. *J. Chem. Soc., Perkin Trans. 2* **1979**, 1103.

(11) (a) James, D. R.; Siemiarczuk, A.; Ware, W. R. *Rev. Sci. Instrum.* **1992,** *63*, 1710. (b) Ware, W. R.; Watt, D.; Holmes, J. D. *J. Am. Chem Soc.* **1974**, *96*, 7853. (c) Lewis, F. D.; Bassani, D. M. *J. Photochem. Photobiol. A* **1992**, *66*, 43.

(12) Weller, A. *Z. Phys. Chem. (Wiesbaden)* **1982**, *133*, 93.

(13) (a) Lewis, F. D.; Ho, T.-I. *J. Am. Chem. Soc.* **1977**, *99*, 7991. (b) Lewis, F. D.; Correa, P. C. *J. Am. Chem. Soc.* **1984**, *106*, 194.

(14) (a) Van der Auweraer, M.; Grabowski, Z. R.; Rettig, W. *J. Phys. Chem.* **1991**, *95*, 2083. (b) Van Haver, Ph.; Helsen, N.; Depaemelaere, S.; Van der Auweraer, M.; De Schryver, F. C. *J. Am. Chem. Soc.* **1991**, *113*, 6849. (c) Van der Auweraer, M.; Viaene, L.; Van Haver, Ph.; De Schryver, F. C. *J. Phys. Chem.* **1993**, *97*, 7178. (d) Pasman, P.; Mes, G. F.; Koper, N. W.; Verhoeven, J. W. *J. Am. Chem. Soc.* **1985**, *107*, 5839. (e) Wegewijs, B.; Hermant, R. M.; Verhoeven, J. W.; Kunst, A. G. M.; Rettschnick, R. P. H. *Chem. Phys. Lett.* **1987**, *140*, 587. (f) Verhoeven, J. W. *Pure Appl. Chem.* **1990**, *62*, 1585. (g) Lewis, F. D.; Bassani, D. M.; Burch, E. L.; Cohen, B. E.; Engelman, J. A.; Reddy, G. D.; Schneider, S.; Gahr, M. *J. Am. Chem. Soc.* **1994**, *116*, 597. (h) Lewis, F. D.; Reddy, G. D.; Bassani, D. M.; Schneider, S.; Jaeger, W.; Gedeck, P.; Gahr, M. *J. Am. Chem. Soc.* **1994**, *116*, 597.

(15) Amide *E,Z* photoisomerization has been observed for nonconjugated secondary amides. See the following. (a) Wang, Y.; Purrello, R.; Spiro, T. G. *J. Am. Chem. Soc.* **1989**, *111*, 8274. (b) Song, S.; Asher, S. A.; Krimm, S.; Shaw, K. D. *J. Am. Chem. Soc.* **1991**, *113*, 1155.

(16) de Silva, A. P.; Gunaratne, H. Q. N.; Habib-Jiwan, J.-L.; McCoy, C. P.; Rice, T. E.; Soumillion, J.-P. *Angew. Chem., Int. Ed. Engl.* **1995,** *34*, 1728.

(17) INDO/S calculations indicate that the LUMO of **14** has delocalized enonecharacter but that the carbonyl π-orbial coefficients for the other frontier orbitals of **1**, **4**, and **14** are insignificant.[6]

(18) For the use of piperidines as semirigid spacers see the following. Schuddeboom, W.; Scherer, T.; Warman, J. M.; Verhoeven, J. W. *J. Phys. Chem.* **1993**, *97*, 13092.

(19) The oxidation potentials of Et_3N and *N*-methylpiperidine are 1.42 and 1.28 V, respectively.

(20) (a) Brouwer, A. M.; Langkilde, F. W.; Bajdor, K.; Wilbrandt, R. *Chem. Phys. Lett.* **1994**, *225*, 386. (b) Jacques, P.; Allonas, X. *Chem. Phys. Lett.* **1995**, *233*, 533.

(21) (a) Oliver, A. M.; Craig, D. C.; Paddon-Row, M. N.; Kroon, J.; Verhoeven, J W. *Chem. Phys. Lett.* **1988**, *150*, 366. (b) Borovkov, V. V.; Ishida, A.; Takamuku, S.; Sakata, Y. *Chem. Lett.* **1993**, 737.

(22) Sugimoto, A.; Sumida, R.; Tamai, N.; Inoue, H.; Otsuji, Y. *Bull. Chem. Soc. Jpn.* **1981**, *54*, 3500.

(23) Lewis, F. D.; Cohen, B. E. *J. Phys. Chem.* **1994**, *98*, 10591.

(24) (a) Wasielewski, M. R.; Minsek, D. W.; Niemczyk, M. P.; Svec, W. A.; Yang, N. C. *J. Am. Chem Soc.* **1990**, *112*, 2823. (b) Rettig, W.; Haag, R.; Wirz, J. *Chem. Phys. Lett.* **1991**, *180*, 216.

(25) Helsen, N.; Viaene, L.; Van der Auweraer, M.; De Schryver, F. C. *J. Phys. Chem.* **1994**, *98*, 1532.

(26) Lippert, E. *Z. Naturforscher* **1955**, *109*, 541. (b) Mataga, N.; Kaifu, Y.; Koizumi, M. *Bull. Chem. Soc. Jpn.* **1955**, *28*, 690.

(27) Swinnen, A. M.; Van der Auweraer, M.; De Schryver, F. C.; Nakatani, K.; Okada, T.; Mataga, N. *J. Am. Chem. Soc.* **1987**, *109*, 321.

(28) Okada, T.; Mataga, N. *Bull. Chem. Soc. Jpn* **1976**, *49*, 2190.

(29) Piuzzi, F.; Brenner, V.; Millié, P.; Tramer, A. *J. Photochem. Photobiol. A* **1994**, *80*, 95.

(30) (a) Reynders, P.; Kühnle, W.; Zachariasse, K. *J. Am. Chem. Soc.* **1990**, *112*, 3928. (b) Kawakami, J.; Iwamura, M.; Nakamura, J. *Chem. Lett.* **1992**, 1013. (c) Yu, H.-T.; Vela, M. A.; Fronczek, F. R.; McLaughlin, M. L.; Barkley, M. D. *J. Am. Chem. Soc.* **1995**, *117*, 348.

(31) Itoh, H.; Takada, M.; Asano, F.; Senda, Y.; Sakuragi, H.; Tokumaru, K. *Bull. Chem. Soc. Jpn.* **1993**, *66*, 224.

(32) Berlman, I. B. *Fluorescence Spectra of Aromatic Molecules*; Academic Press: New York, 1971.

(33) For a full description see the following. Bordwell, F. G.; Cheng, J.-P.; Bausch, M. J. *J. Am. Chem. Soc.* **1988**, *110*, 2867.

(34) Wilson, W. D.; Wang, Y.-H.; Kusuma, S.; Chandrasekaran, S.; Boykin, D. W. *Biophys. Chem.* **1986**, *24*, 101.

(35) Sheehan, J. C.; Hess, G. P. *J. Am. Chem. Soc.* **1955**, *77*, 1067.

JP9526758